NACA RM L51F08a

NACA

RESEARCH MEMORANDUM

SMALL-SCALE INVESTIGATION AT TRANSONIC SPEEDS OF THE EFFECTS OF THICKENING THE INBOARD SECTION OF A 45° SWEPTBACK WING OF ASPECT RATIO 4, TAPER RATIO 0.3, AND NACA 65A006 AIRFOIL SECTION

By Kenneth P. Spreemann and William J. Alford, Jr.

Langley Aeronautical Laboratory
Langley Field, Va.

NATIONAL ADVISORY COMMITTEE
FOR AERONAUTICS

WASHINGTON

August 9, 1951

NACA RM L51F08a

NATIONAL ADVISORY COMMITTEE FOR AERONAUTICS

RESEARCH MEMORANDUM

SMALL-SCALE INVESTIGATION AT TRANSONIC SPEEDS OF THE EFFECTS OF THICKENING THE INBOARD SECTION OF A 45° SWEPTBACK WING OF ASPECT RATIO 4, TAPER RATIO 0.3, AND NACA 65A006 AIRFOIL SECTION

By Kenneth P. Spreemann and William J. Alford, Jr.

SUMMARY

A small-scale investigation was conducted in the Langley high-speed 7- by 10-foot tunnel over a range of Mach numbers from 0.60 to 1.08 to determine the effects of increasing the thickness ratio over the inboard portion of the span of a wing with the quarter-chord line sweptback 45°. The investigation included tests of a basic wing having a constant 6-percent-thick section and a modification of this wing having the section thickness increased from 6 percent at the 40-percent-semispan station to 12 percent at the root.

The wing with thickened inboard section gave large increases in minimum drag in the transonic speed range. The lift-curve slope, lateral center of pressure, and aerodynamic-center location were only slightly affected by modifying the wing. Experimental values of lift-curve slope, lateral center of pressure, and aerodynamic-center location appeared to be in good agreement with theoretical values (corrected to the elastic conditions) in the low-supersonic Mach number range. In the subsonic Mach number range the experimental values of these parameters were in reasonably good agreement with the theoretical values except for the aerodynamic-center location.

INTRODUCTION

It is desirable for structural reasons to maintain the airplane wing-thickness ratio at as large a value as feasible without incurring great penalties in performance and in stability and control characteristics at

transonic speeds. The investigation reported in reference 1 indicated that full-span tapering of thickness ratio offered a possible means of improving the structural characteristics without noticeable sacrifices in the aerodynamic characteristics. It was subsequently proposed that the structural advantages of thick root sections and the aerodynamic advantages of thin tip sections might be achieved, at least in part, by increasing the thickness ratio over only a limited inboard portion of the wing span.

The aerodynamic effects of increasing thickness ratio of the inboard portion of a representative 45° sweptback wing of aspect ratio 4 are presented in this paper. The investigation included two semispan wings, one a wing of 6-percent constant thickness and the other (a modification of the first wing) having the inboard portion tapered in thickness from 6 percent at the 40-percent-semispan station to 12 percent at the wing root. Lift, drag, pitching moment, and root bending moment were obtained over a Mach number range from 0.60 to 1.08 in the Langley high-speed 7- by 10-foot tunnel. Also, some comparisons were made with theoretical values, corrected to elastic conditions, at subsonic and low-supersonic speeds.

SYMBOLS

The symbols used in this paper are defined as follows:

C_L lift coefficient (Twice semispan lift/qS)

C_D drag coefficient (Twice semispan drag/qS)

C_m pitching-moment coefficient referred to $0.25\bar{c}$ (Twice semispan pitching moment/$qS\bar{c}$)

C_B bending-moment coefficient about axis parallel to relative wind and in plane of symmetry $\left(\frac{\text{Root bending moment}}{q\frac{S}{2}\frac{b}{2}}\right)$

ΔC_D drag coefficient due to lift $\left(C_D - C_{D_{C_L=0}}\right)$

$\frac{c_l c}{C_L c_{av}}$ span load coefficient

c_l section lift coefficient

D_F equivalent leading-edge-suction factor $\left(100\left(\frac{\frac{C_{L_\alpha}}{57.3} - \Delta C_D}{\frac{C_{L_\alpha}}{57.3} - C_{D_i}}\right)\right)$

C_{D_i} theoretical induced-drag coefficient $\left(1.0025 \frac{C_L^2}{\pi A}\right.$, calculated by method of reference 3$)$

A aspect ratio $\left(\frac{b^2}{S}\right)$

q effective dynamic pressure over span of model, pounds per square foot $\left(\frac{1}{2}\rho V^2\right)$

S twice wing area of semispan model, 0.125 square foot

$\bar{c}$ mean aerodynamic chord of wing, 0.181 foot; based on relationship $\frac{2}{S}\int_0^{b/2} c^2 dy$ (using theoretical tip)

c local wing chord, feet

c_{av} average wing chord, feet

b twice span of semispan model, 0.707 foot

y spanwise distance from plane of symmetry, feet

ρ air density, slugs per cubic foot

V stream velocity over model, feet per second

M effective Mach number over span of model

M_l local Mach number

M_a average chordwise Mach number

R	Reynolds number $(\rho V\bar{c}/\mu)$
μ	absolute viscosity, pound-seconds per square foot
E	Young's modulus of elasticity, pounds per square inch
α	angle of attack, degrees
α_D	local angle of streamwise wing twist, degrees
x	chordwise distance from leading edge of root chord to wing aerodynamic center, feet
l	chordwise distance from leading edge of root chord to quarter-chord point of mean aerodynamic chord, feet
y_{cp}	lateral center of pressure, percent semispan $\left(100 \frac{\partial C_B}{\partial C_L}\right)$
t	wing thickness, feet

MODELS AND TESTS

The modified wing of the present investigation was obtained by altering a basic semispan wing model, which had 45° of sweepback referred to the quarter-chord line, an aspect ratio of 4, a taper ratio of 0.3, and an NACA 65A006 airfoil section parallel to the free stream. The modification consisted of thickening the inboard portion of the wing to provide an NACA 65A012 airfoil section at the root, tapered to the basic NACA 65A006 airfoil section at the 40-percent-semispan station. The original wing was made of beryllium-copper and the modification was constructed of bismuth-tin alloy. A drawing of the wing, including the modification, is shown in figure 1. A photograph of the wing mounted on the reflection-plane plate is shown in figure 2. The distribution of maximum thickness along the semispan is shown in figure 3.

The investigation was conducted in the Langley high-speed 7- by 10-foot tunnel with the model mounted on a reflection-plane plate (fig. 1) located 3 inches from the tunnel wall in order to bypass the wall boundary layer. The reflection-plane boundary-layer thickness was such that a value of 95 percent of free-stream velocity was reached at a distance of approximately 0.16 inch from the surface at the center line of the balance for all test Mach numbers. This boundary-layer thickness represented a distance of about 4 percent semispan for the models tested.

At Mach numbers below 0.95, there was practically no velocity gradient in the vicinity of the reflection plane. At higher Mach numbers, however, the presence of the reflection-plane plate created a high-local-velocity field which allowed testing the small models up to M = 1.08 before choking occurred in the tunnel. The variations of local Mach numbers are shown in figure 4. Effective test Mach numbers were obtained from additional contour charts similar to those shown in figure 4 by the relationship

$$M = \frac{2}{S}\int_0^{b/2} cM_a \, dy$$

For the models tested, outside the boundary layer, a Mach number gradient of generally less than 0.02 was obtained between Mach numbers of 0.95 and 1.04, and the gradient increased to about 0.06 at the highest test Mach number of 1.08. It will be noted that the Mach number gradient is principally chordwise.

Force and moment measurements were made for the models through a Mach number range of 0.60 to 1.08 and an angle-of-attack range of -6° to 12°; the variation of Reynolds number with Mach number for these tests is shown in figure 5. Data were obtained by using a strain-gage balance system. The models were tested with the quarter mean aerodynamic chord located at the center line of the balance, so that transfers to the pitching moments were unnecessary. However, the bending moments were measured about the 7-percent-semispan station and were transferred to the root chord. A gap of about 1/16 inch was maintained between the wing-root-chord section and the turntable of the reflection-plane plate, and a sponge-wiper seal was fastened to the wing butt to minimize leakage.

In view of the small size of the models relative to the tunnel test section, jet-boundary and blockage corrections were believed to be insignificant and were not applied to the data.

THEORETICAL CONSIDERATIONS

Incompressible aerodynamic characteristics were calculated by the discrete vortex method of reference 2. The locations of the lateral center of pressure and the aerodynamic center were assumed to be invariant at subcritical speeds, but the lift-curve slopes were corrected for compressibility by use of the charts in reference 3. The aerodynamic characteristics at low-supersonic speeds were determined by means of

the linearized theory of reference 4. All the theoretical parameters were corrected by strip-theory methods to an elastic condition by using the values of average streamwise twist (fig. 6), obtained by simple beam theory. The equations used for these corrections are summarized as follows:

$$C_{L_\alpha} = C_{L_a}' \int_0^1 \left(1 + \frac{\alpha_D}{qC_L} qC_{L_\alpha}'\right) \frac{c_l c}{C_L c_{av}} d\left(\frac{y}{b/2}\right) \tag{1}$$

$$y_{cp} = \frac{C_{L_\alpha}'}{C_{L_\alpha}} \int_0^1 \left(1 + \frac{\alpha_D}{qC_L} qC_{L_\alpha}'\right) \frac{c_l c}{C_L c_{av}} \frac{y}{b/2} d\left(\frac{y}{b/2}\right) \tag{2}$$

$$\frac{\partial C_m}{\partial C_L} = \frac{l - x}{\bar{c}} \tag{3a}$$

$$\frac{x}{\bar{c}} = \frac{C_{L_\alpha}'}{C_{L_\alpha}} \int_0^1 \left(1 + \frac{\alpha_D}{qC_L} qC_{L_\alpha}'\right) \frac{c_l c}{C_L c_{av}} \frac{x_l}{\bar{c}} d\left(\frac{y}{b/2}\right) \tag{3b}$$

where

C_{L_α} theoretical lift-curve slope for elastic wing

C_{L_α}' theoretical lift-curve slope for rigid wing

x_l distance from root leading edge to local aerodynamic center, feet (assumed to be at $c/4$ for subsonic Mach numbers)

The increase in drag coefficient for the modified wing from the subsonic Mach number range (below $M = 0.80$) to the supersonic Mach number range (above Mach numbers of 1.04) was estimated by use of the following equation:

$$C_{D_2} = \frac{C_{D_1}}{\left(t_1/c\right)^2} \int_0^1 \frac{c}{c_{av}} \left(\frac{t_2}{c}\right)^2 d\left(\frac{y}{b/2}\right) \tag{4}$$

where, for example:

C_{D_1} increase in drag coefficient for the basic wing between M = 0.80 and M = 1.05 (from experimental results)

C_{D_2} estimated increase in drag coefficient for modified wing between M = 0.80 and M = 1.05

t_1/c thickness ratio of basic wing (0.06)

t_2/c thickness ratio of modified wing (see fig. 3)

The remainder of the coefficients and symbols have been previously defined.

RESULTS AND DISCUSSION

The basic data of the investigation are shown in figure 7. The discussion is based principally on the summary curves presented in figure 8. The slopes presented in figure 8 were measured through zero lift up to a lift coefficient where obvious departures from linearity occurred.

Lift and Drag Characteristics

The lift-curve slopes $\partial C_L/\partial\alpha$ were reduced about 0.003 in the subsonic speed range and about 0.006 in the supersonic speed range by modifying the thickness ratio of the inboard portion of the wing. The difference in $\partial C_L/\partial\alpha$ of the two wings probably can be attributed primarily to the low Reynolds numbers of this investigation (see, for example, reference 5). The lift-curve slopes of both wings at subsonic Mach numbers were higher than indicated by theory corrected to the elastic conditions. However, in the supersonic Mach number range the theoretical calculations for the elastic conditions appeared to predict quite well the extrapolated lift-curve slope of the basic wing. The lift-curve slopes of the wing in reference 6 (in which the same basic wing was employed as for the present investigation) were about 0.005 to 0.009 lower than those of this investigation. The lower values of $\partial C_L/\partial\alpha$ possibly may be attributed to leakage of air around the butt of the model and to end-plate tares, as these factors were not accounted for in the investigation of reference 6. In the present investigation,

these conditions were to a large extent avoided by installing a sponge-wiper seal at the butt of the model and eliminating the end plate.

The wing modification gave a 2 to 3 percent outboard movement of the lateral center of pressure in the lower Mach number range. It should be pointed out that the lateral center-of-pressure locations presented in this paper are based only on the bending moment due to lift; however, within the low-lift-coefficient range in which the slopes of the bending moments were measured, drag would have very little effect on the bending moments. It is interesting to note that the theoretical calculations for the elastic conditions in the subsonic speed range almost precisely predicted the lateral center of pressure of the modified wing. In the supersonic region the theory gave lateral center-of-pressure values that appear to be just slightly outboard of those that might be extrapolated from the experimental results of either wing.

The modified wing showed considerably higher drag values than the original wing in the transonic speed range, as evidenced by the large increases in $C_{D_{min}}$ above a Mach number of 0.95. The comparatively large differences in $C_{D_{min}}$ at the lower Mach numbers may be the result of the low Reynolds number of this investigation. The Reynolds number effects given in reference 5 show that as the Reynolds numbers are increased to values above 5×10^6 the differences in $C_{D_{min}}$ between wings of these thickness ratios are very small (about 0.0007 at a Reynolds number of 8×10^6, compared with a value of about 0.0025 indicated at a Reynolds number of 0.75×10^6 in the present investigation). The rise in drag coefficient for the modified wing between $M = 0.80$ and $M = 1.05$, as estimated by use of equation 4, was in good agreement with experiment, as shown in figure 8. It is also of interest to note that the drag-rise Mach number was somewhat reduced by modifying the wing.

The parameter D_F (fig. 8) represents the percent of equivalent full leading-edge suction realized at the various lift coefficients. It should be noted that the percent of equivalent leading-edge suction indicated by D_F is undoubtedly conservative, inasmuch as the drag due to lift may be increased by trailing-edge separation as well as by losses in leading-edge suction. At low lift coefficients (0.2 and lower) the drag due to lift ΔC_D was apparently little affected by the wing modification. The values of ΔC_D obtained at these low lift coefficient below $M = 1.0$ correspond to the achievement of about 60 to 80 percent of the equivalent full leading-edge suction, and up to where compressibility effects might be more pronounced, the thicker, modified wing

showed slightly higher values of D_F. At a lift coefficient of 0.6, ΔC_D was increased about 0.004 to 0.010 by the wing modification. Nevertheless, in the lower Mach number range, D_F was about the same for both wings at $C_L = 0.6$ (about 35 to 40 percent of the equivalent full leading-edge suction). This can be attributed to the lower average lift-curve slope of the modified wing.

The maximum lift-drag ratios were very adversely influenced by modifying the inboard wing thickness. The reductions in maximum lift-drag ratios were about 17 percent at low Mach numbers and increased to about 27 percent at the highest Mach numbers. It should be noted that at subcritical Mach numbers most of the losses in maximum lift-drag ratios were probably attributable to the aforementioned Reynolds number effects on $C_{D_{min}}$. The greater percentage reductions of $(L/D)_{max}$ in the speed range above $M = 0.90$ may be primarily attributed to the large increases in $C_{D_{min}}$ in this speed range.

Pitching-Moment Characteristics

The pitching-moment characteristics (fig. 7) were only slightly influenced by modifying the inboard wing thickness. The values of $\partial C_m / \partial C_L$ in figure 8 show that forward movements of the aerodynamic-center location of about 1.0 to 2.5 percent of the mean aerodynamic chord were obtained as a result of the wing modification. Inasmuch as the lateral center of pressure of the modified wing was outboard of that of the basic wing, the more forward location of the aerodynamic center on the modified wing is probably attributable to a more forward chordwise location of the local aerodynamic center on the inboard portion of the wing. The theoretical values of $\partial C_m / \partial C_L$ indicated an aerodynamic-center location about 5 or 6 percent of the mean aerodynamic chord ahead of those obtained experimentally in the subsonic Mach number range. In the supersonic Mach range investigated, however, the theoretical calculations seemed to predict the extrapolated experimental aerodynamic-center location of the basic wing quite well.

CONCLUSIONS

A small-scale investigation of the effects of increasing the thickness ratio over the inboard wing sections of a 45° sweptback wing indicated the following:

1. The minimum drag of the modified wing was considerably higher at high-subsonic and low-supersonic speeds than that of the basic wing. The transonic minimum drag rise of the modified wing was closely predicted by simple theory utilizing the minimum drag rise of the original wing determined experimentally in the transonic Mach number range. The drag due to lift at high lift coefficients for the modified wing was generally greater than for the basic wing.

2. No large effects of the wing modification were shown on the variations of lift-curve slope, lateral center of pressure, and aerodynamic-center location with Mach number.

3. The extrapolated experimental lift-curve slope, lateral center of pressure, and aerodynamic-center location agreed very well with theoretical values predicted by linearized theory at low-supersonic speeds. At subsonic speeds the experimental and theoretical values were generally in reasonably good agreement except for the aerodynamic-center location.

Langley Aeronautical Laboratory
National Advisory Committee for Aeronautics
Langley Field, Va.

REFERENCES

1. Morrison, William D., Jr., and Fournier, Paul G.: Effects of Spanwise Thickness Variation on the Aerodynamic Characteristics of 35° and 45° Sweptback Wings of Aspect Ratio 6. Transonic-Bump Method. NACA RM L51D19, 1951.

2. Campbell, George S.: A Finite-Step Method for the Calculation of Span Loadings of Unusual Plan Forms. NACA RM L50L13, 1951.

3. DeYoung, John, and Harper, Charles W.: Theoretical Symmetric Span Loading at Subsonic Speeds for Wings Having Arbitrary Plan Form. NACA Rep. 921, 1948.

4. Cohen, Doris: Formulas and Charts for the Supersonic Lift and Drag of Flat Swept-Back Wings with Interacting Leading and Trailing Edges. NACA TN 2093, 1950.

5. Jacobs, Eastman N., and Sherman, Albert: Airfoil Section Characteristics as Affected by Variations of the Reynolds Number. NACA Rep. 586, 1937.

6. Myers, Boyd C., II., and King, Thomas J., Jr.: Aerodynamic Characteristics of a Wing with Quarter-Chord Line Swept Back 45°, Aspect Ratio 4, Taper Ratio 0.3, and NACA 65A006 Airfoil Section. Transonic-Bump Method. NACA RM L9E25, 1949.

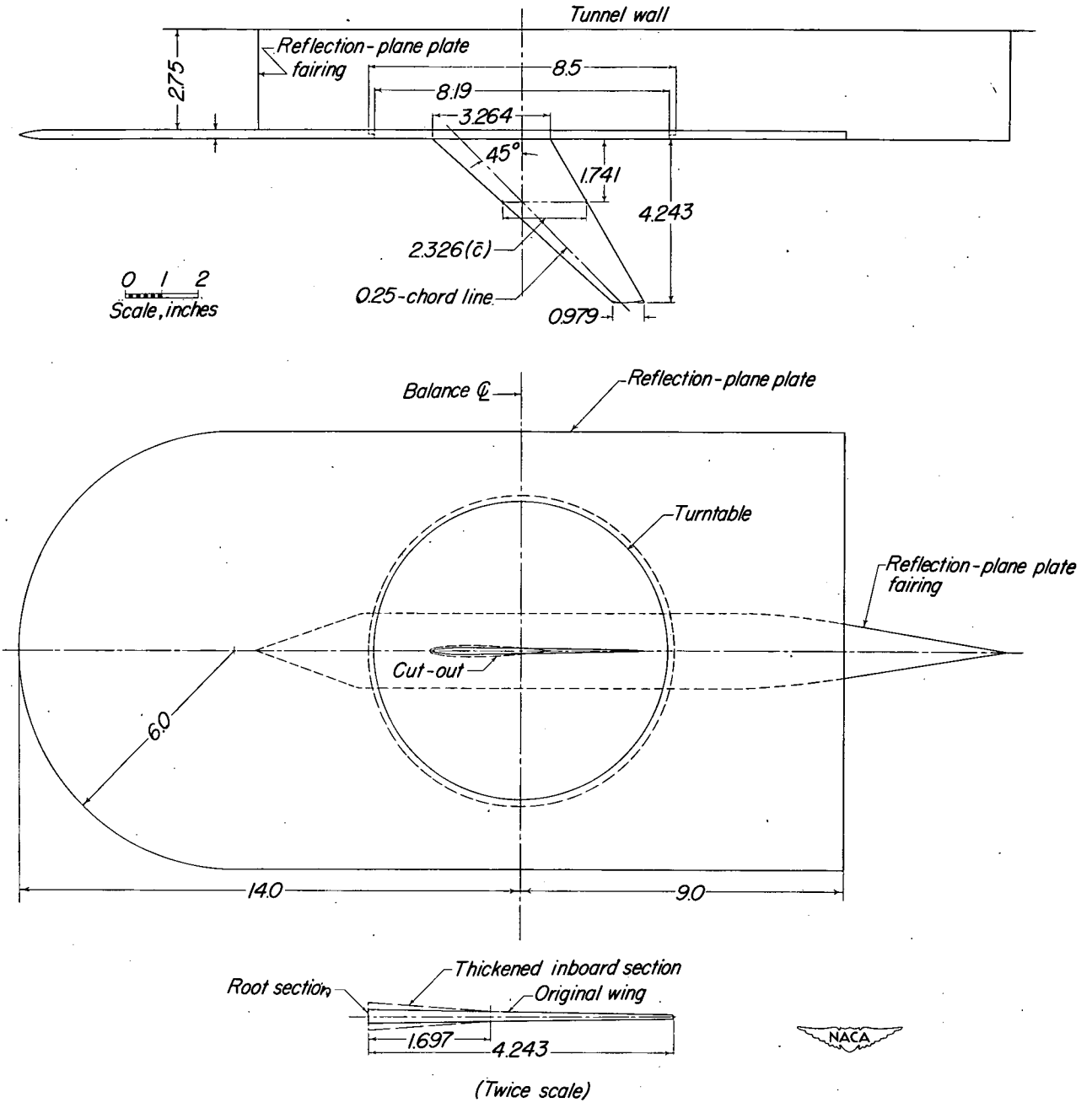

Figure 1.- Test model mounted on the reflection plane in the Langley high-speed 7- by 10-foot tunnel.

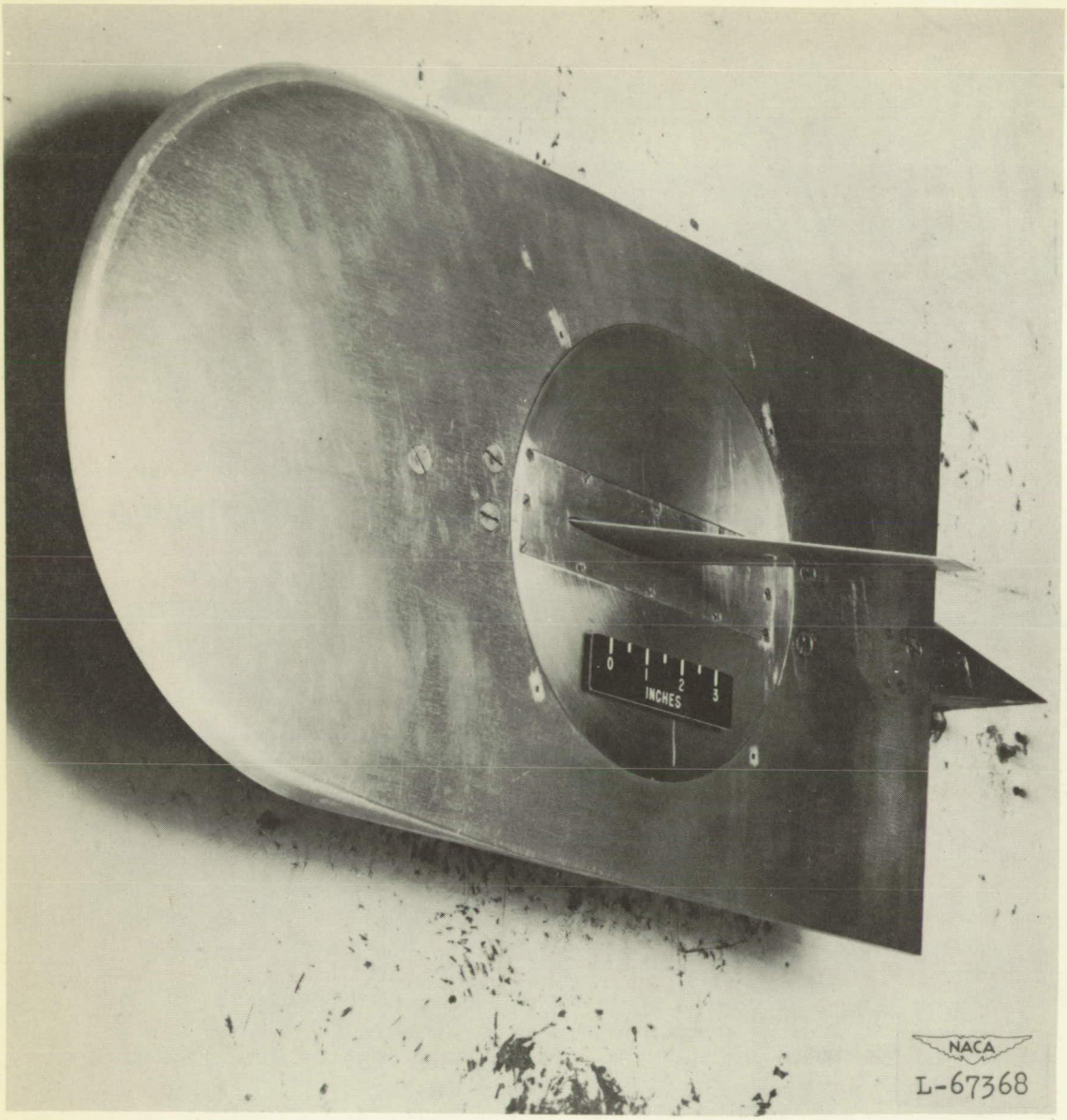

Figure 2.- View of test model mounted on the reflection plane in the Langley high-speed 7- by 10-foot tunnel.

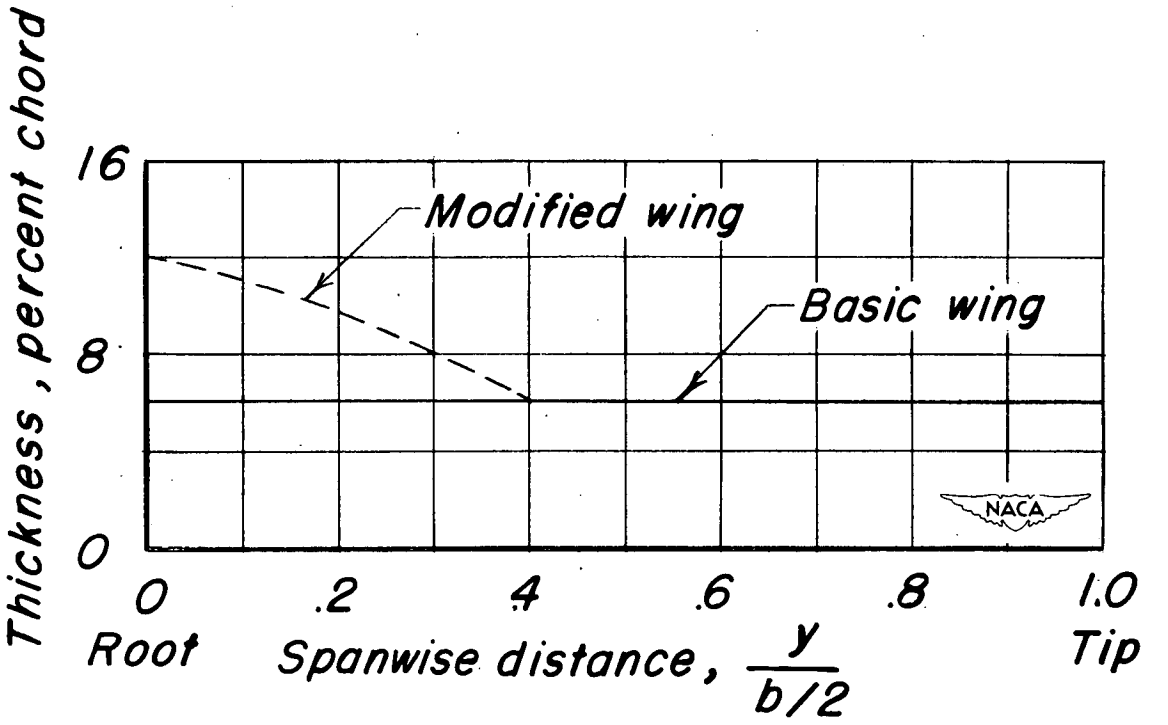

Figure 3.- Maximum-thickness distribution along the semispan of the test models.

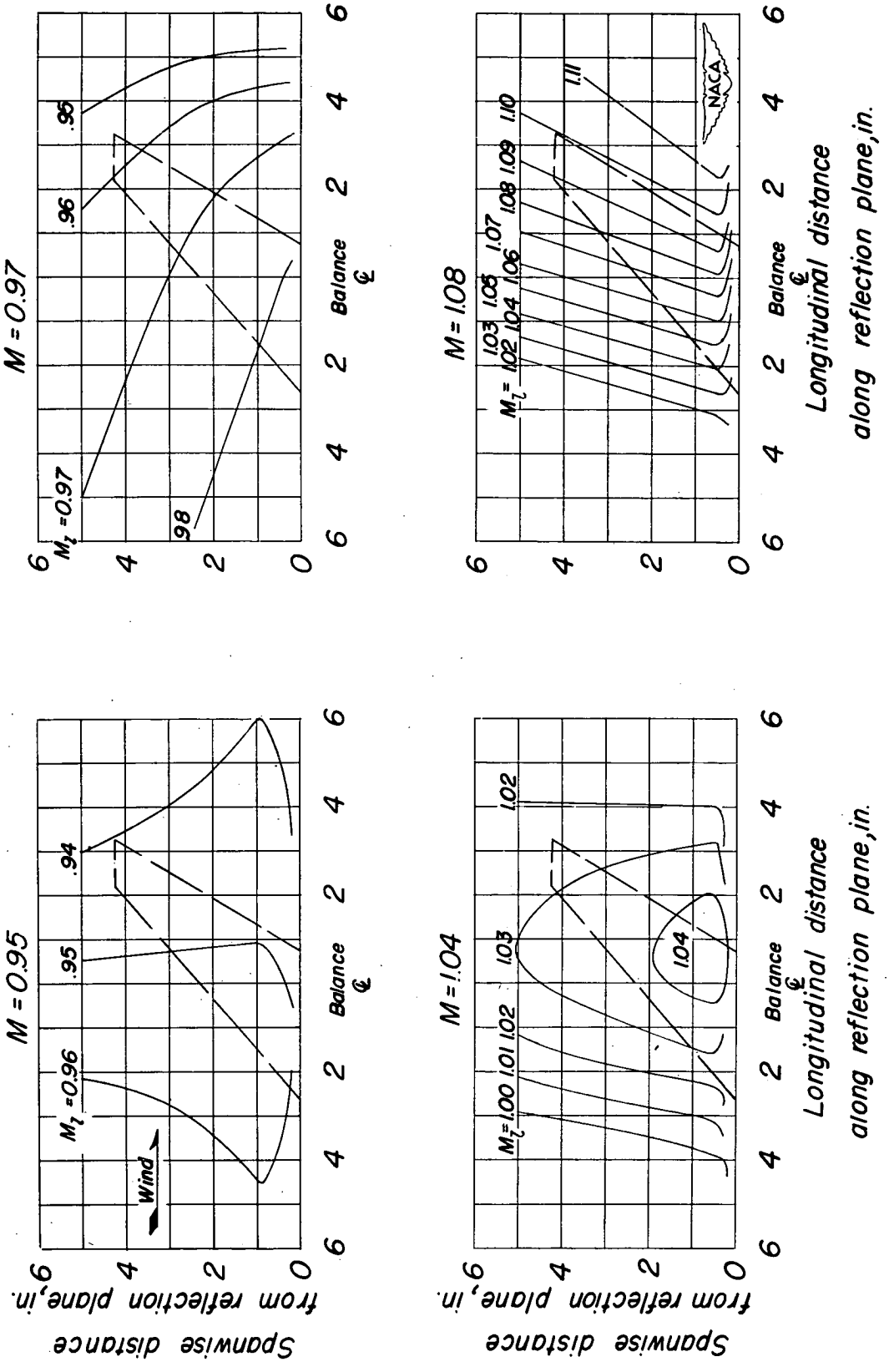

Figure 4.- Typical Mach number contours over side-wall reflection plane in region of model.

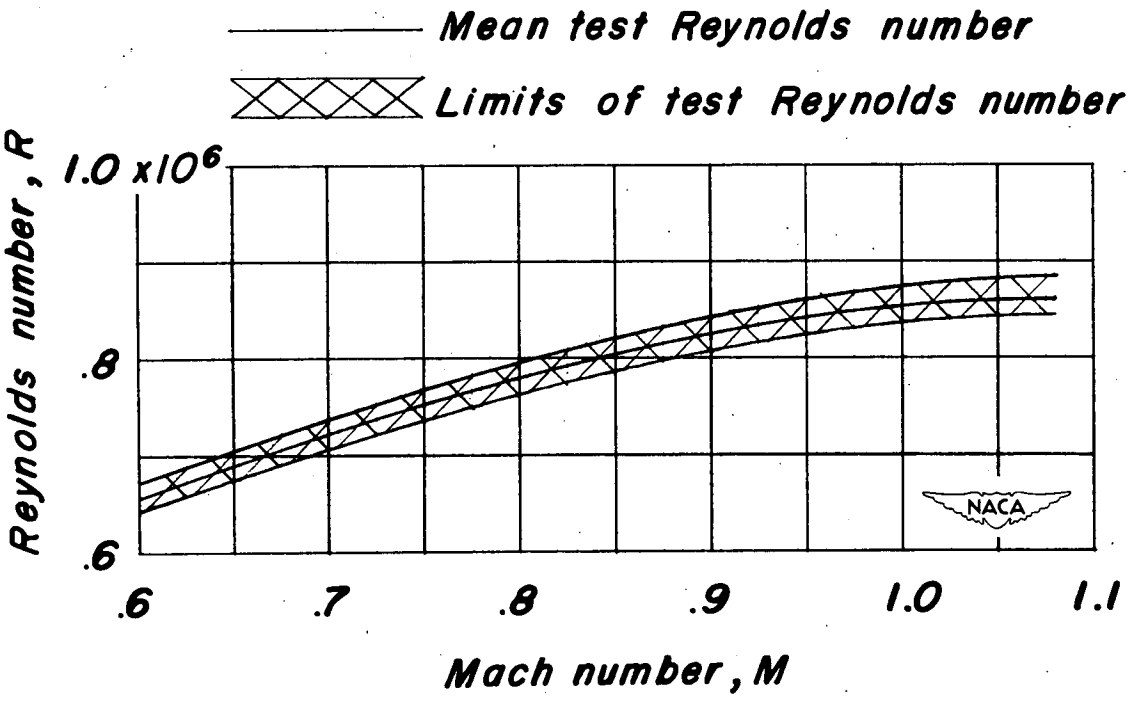

Figure 5.- Variation of test Reynolds number with Mach number for the test models.

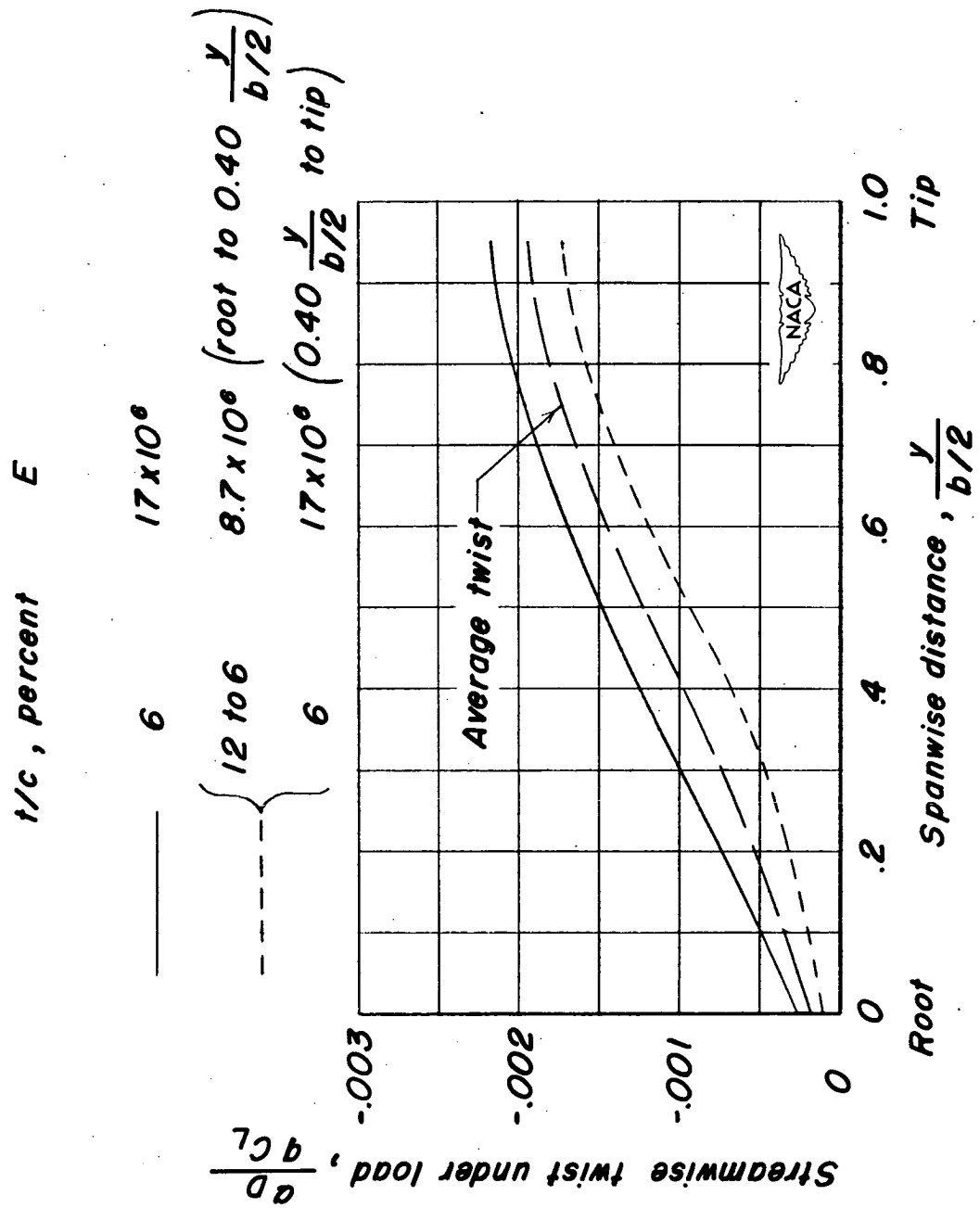

Figure 6.- Calculated streamwise wing twist of test models.

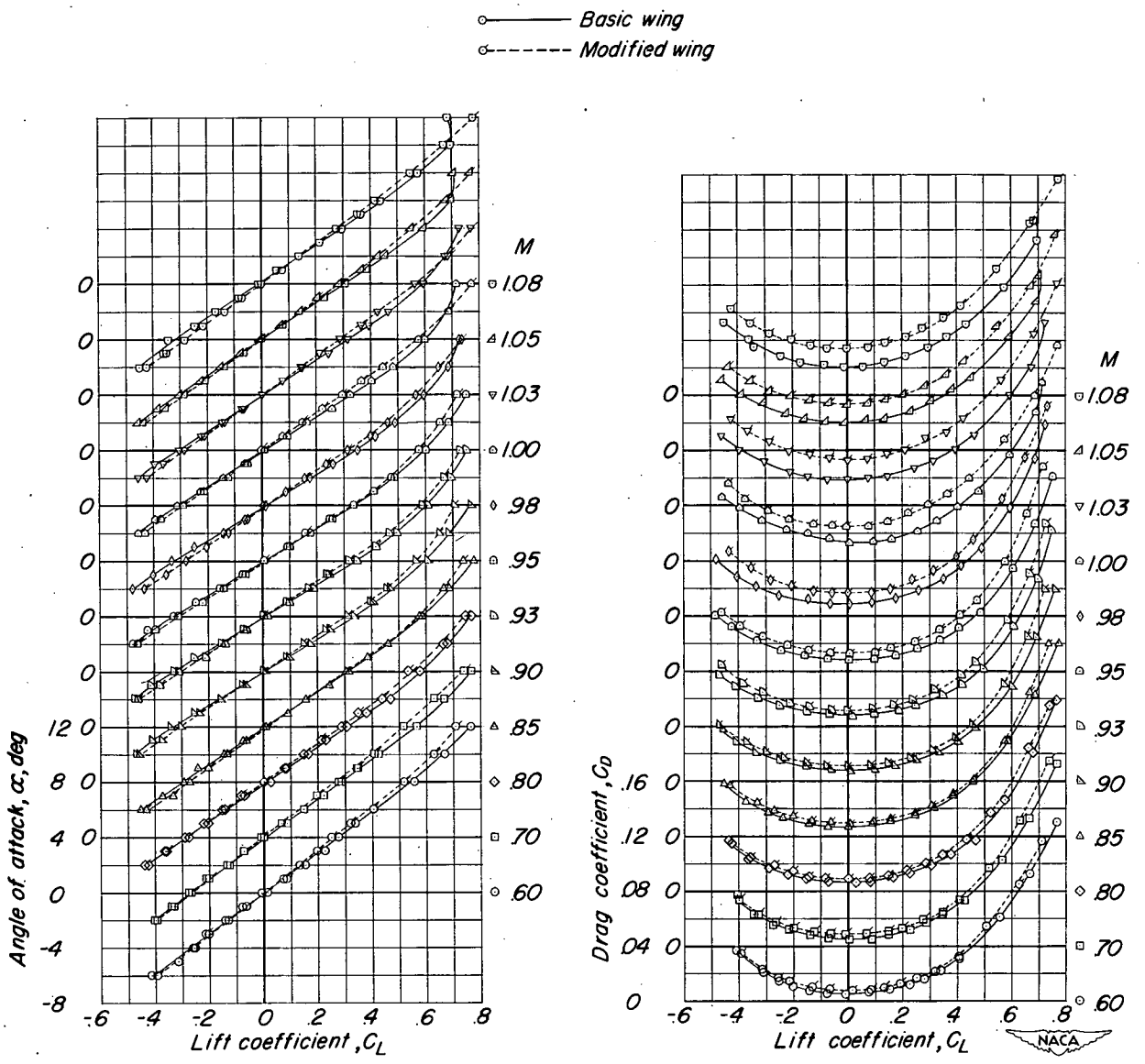

Figure 7.- Aerodynamic characteristics of the test models.

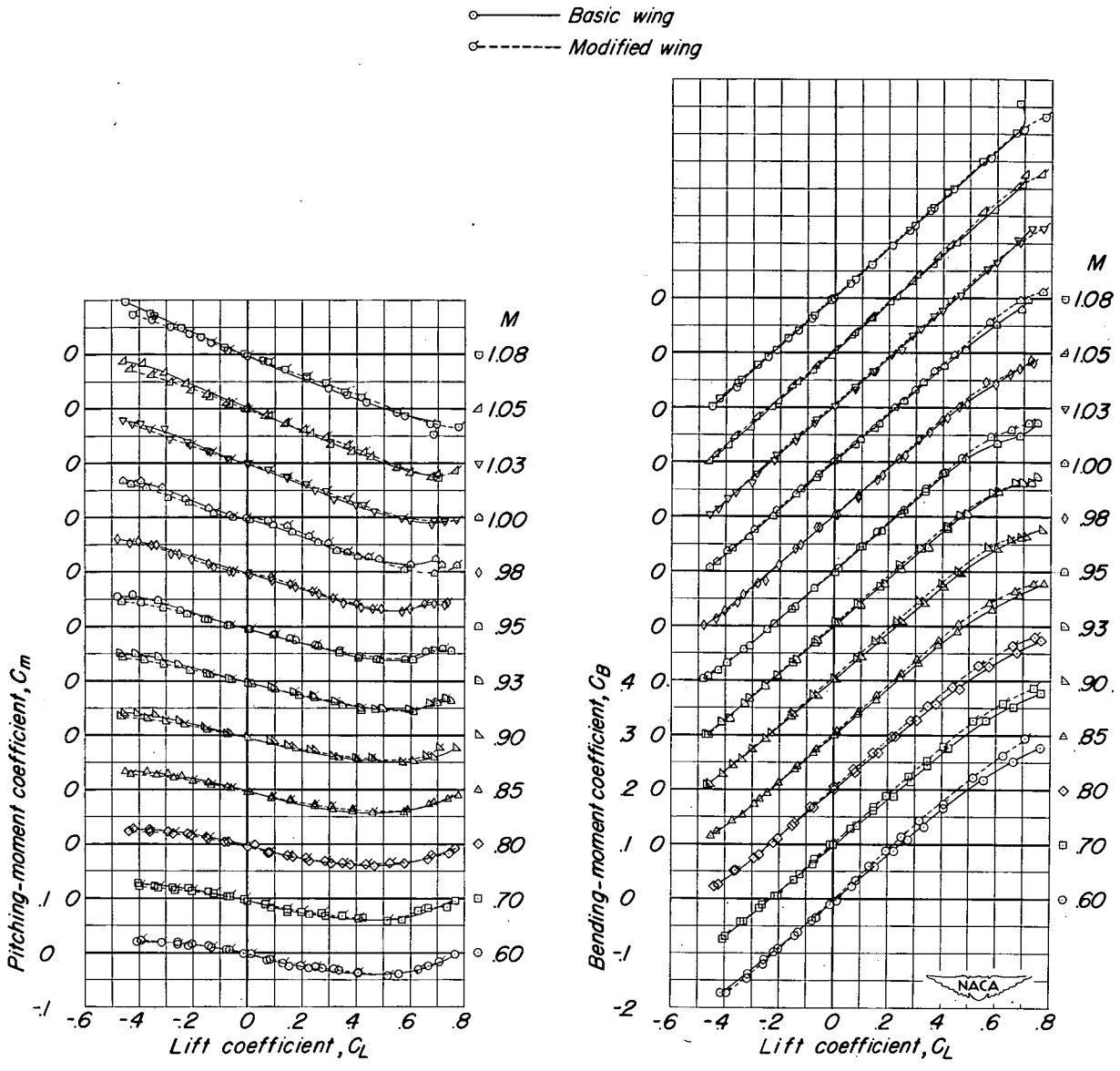

Figure 7.- Concluded.

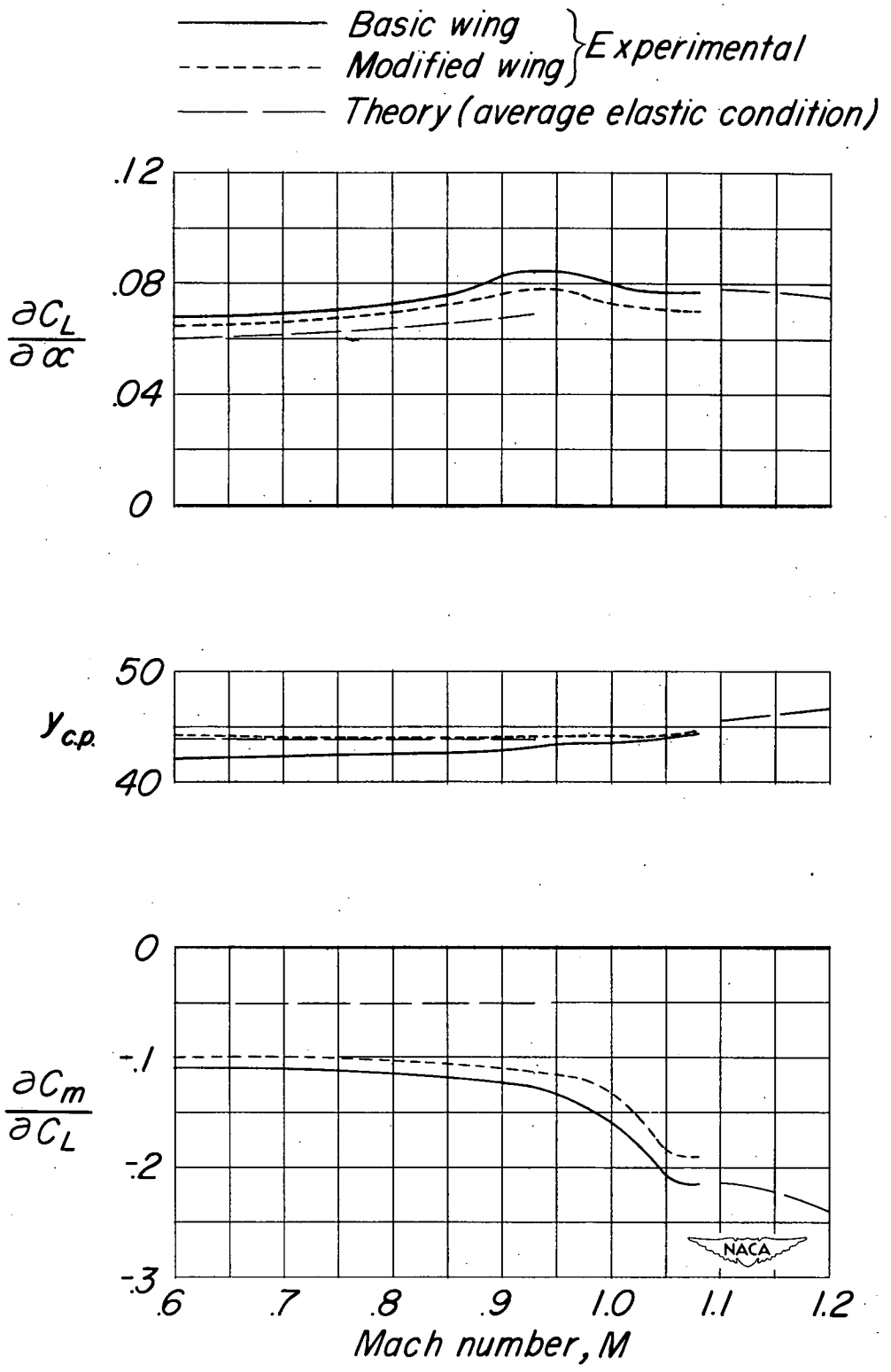

Figure 8.- Summary of aerodynamic characteristics of the test models.

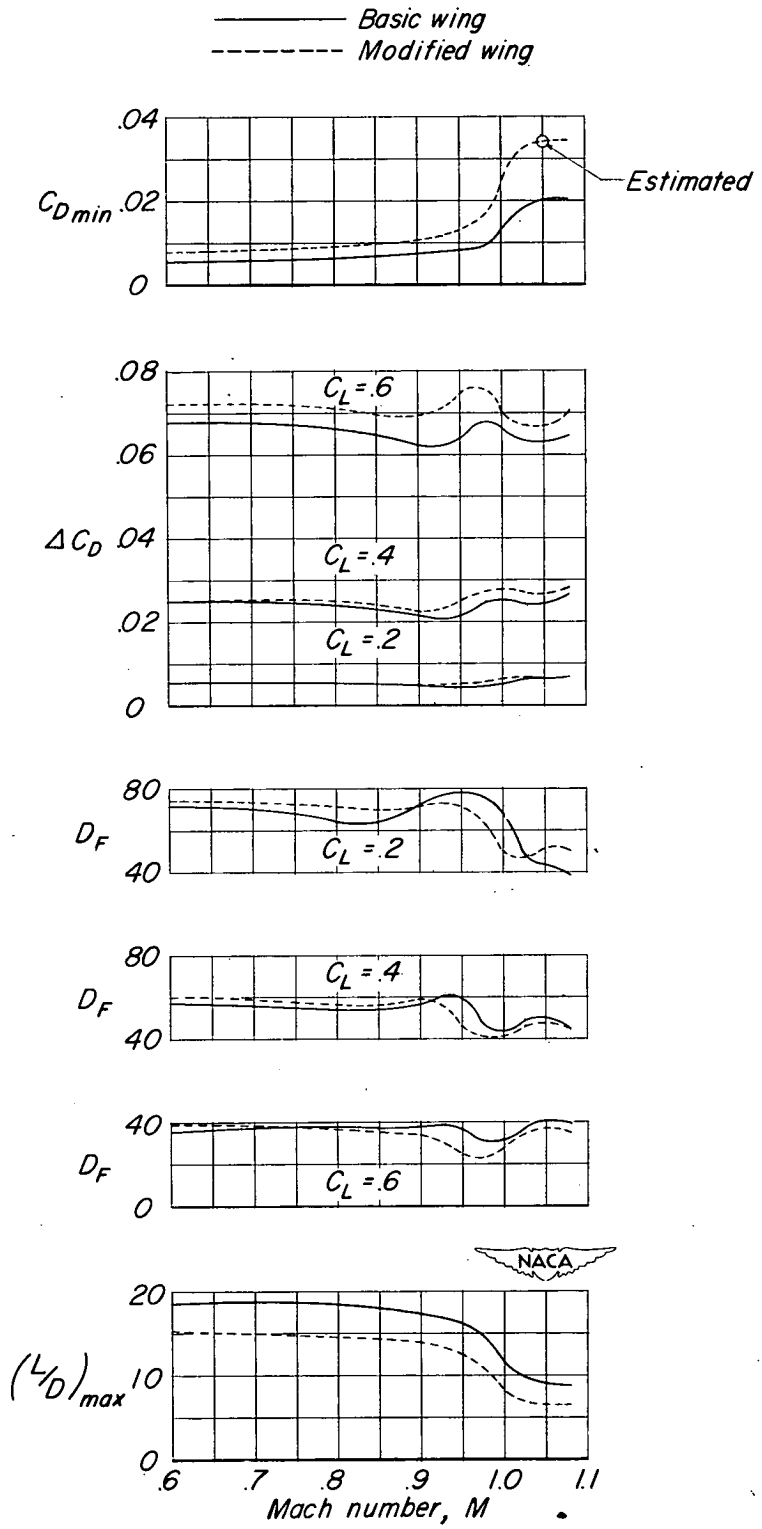

Figure 8.- Concluded.